Published in final edited form as:
Nature. 2014 January 16; 505(7483): 367–371. doi:10.1038/nature12867.

Biochemical reconstitution of topological DNA binding by the cohesin ring

Yasuto Murayama and **Frank Uhlmann**
Chromosome Segregation Laboratory, Cancer Research UK London Research Institute, 44 Lincoln's Inn Fields, London WC2A 3LY, UK

Abstract

Cohesion between sister chromatids, mediated by the chromosomal cohesin complex, is a prerequisite for faithful chromosome segregation in mitosis. Cohesin plays vital roles also in DNA repair and transcriptional regulation. The ring-shaped cohesin complex is thought to encircle sister DNA strands, but its molecular mechanism of action is poorly understood and the biochemical reconstitution of cohesin activity *in vitro* has remained an unattained goal. We have now reconstituted cohesin loading onto DNA using purified fission yeast cohesin and its loader complex, Mis4^{Scc2}/Ssl3^{Scc4}. Incubation of cohesin with DNA leads to spontaneous topological loading, but that remains inefficient. The loader contacts cohesin at multiple sites around the ring circumference, including the hitherto enigmatic Psc3^{Scc3} subunit, and stimulates cohesin's ATPase, resulting in efficient topological loading. The *in vitro* reconstitution of cohesin loading onto DNA provides mechanistic insight into the initial steps of establishing sister chromatid cohesion and other chromosomal processes mediated by cohesin.

The cohesin complex is a central player in chromosome biology[1-5]. Defects in cohesin and its regulators are responsible for chromosome missegregation in human cancers and are the cause for Cornelia de Lange syndrome, a severe developmental disorder[6,7]. Despite notable advances[8-10], our molecular understanding of cohesin function remains vague. The cohesin complex consists of a dimer of structural maintenance of chromosomes subunits, Psm1^{Smc1} and Psm3^{Smc3}, long coiled coil proteins that interact at their hinge as well as their ABC-type ATPase head domains to form large proteinaceous rings[11,12]. The head interaction is stabilized by the kleisin subunit Rad21^{Scc1}. Several additional subunits associate with this ring assembly, including the essential Psc3^{Scc3} subunit, whose function remains poorly understood[12-16]. Cohesin is thought to promote sister chromatid cohesion by entrapping replicated sister chromatids within the ring's circumference[17], but how the Mis4^{Scc2}/Ssl3^{Scc4} cohesin loader[18], ATP hydrolysis by cohesin[19,20] and cohesion establishment during S-phase[13,21,22] contribute to topological cohesin loading remains unknown. It also remains unknown whether the roles of cohesin outside of sister chromatid cohesion involve topological DNA binding.

Correspondence and requests for materials should be addressed to F. U. (frank.uhlmann@cancer.org.uk)..

Author Contributions Y. M. designed the study, performed all the experiments, analyzed data and wrote the manuscript. F. U. designed and supervised the study and wrote the manuscript.

The authors declare no competing financial interests.

Europe PMC Funders Author Manuscripts

The cohesin loader binds to DNA

We purified the fission yeast Mis4^{Scc2}/Ssl3^{Scc4} cohesin loader complex after overexpression of its two subunits in fission yeast (Fig. 1a and Extended Data Fig. 1a). We used a similar strategy to purify the large Mis4^{Scc2} subunit by itself. Based on its hydrodynamic properties, Mis4^{Scc2}/Ssl3^{Scc4} is a moderately elongated, heterodimeric protein complex (Fig. 1b and Extended Data Fig. 1b). Because Mis4^{Scc2} contains a putative leucine zipper, we investigated DNA binding of Mis4^{Scc2}/Ssl3^{Scc4}. We detected concentration-dependent DNA binding of Mis4^{Scc2}/Ssl3^{Scc4} to double stranded DNA (dsDNA) (Fig. 1c,d and Extended Data Fig. 1c). Single stranded (ssDNA) was bound poorly, while a Y-fork DNA substrate, mimicking open DNA structures that might exist at some physiological cohesin loading sites, showed no increased affinity compared to dsDNA. The dsDNA preference over ssDNA was confirmed in a competition assay (Extended Data Fig. 1d). DNA binding was strongest at low salt concentrations, but remained detectable under physiological conditions (Extended Data Fig. 1e). The Mis4^{Scc2} subunit alone displayed DNA binding properties indistinguishable from the Mis4^{Scc2}/Ssl3^{Scc4} complex (Fig. 1d and Extended Data Fig. 1d). These results suggest that the cohesin loader makes direct contact with dsDNA and that the Mis4^{Scc2} subunit is largely responsible for it.

Topological cohesin loading *in vitro*

We purified the fission yeast cohesin complex after overexpression of its four essential subunits Psm1, Psm3, Rad21 and Psc3 in budding yeast (Fig. 2a,b and Extended Data Fig. 2a). The complex showed ATP-independent dsDNA binding, as previously reported for cohesin[8,23], that was independent of the substrate topology, but was salt sensitive (Extended Data Fig. 2b,c). Topological DNA binding by cohesin is expected to be salt resistant[10,17,18].

Taking these properties into account, we devised an assay to detect topological cohesin loading onto DNA (Fig. 2c). Cohesin and a relaxed circular DNA (RC DNA) substrate were mixed in the presence of ATP. After incubation, cohesin was immunoprecipitated. The cohesin beads were washed in high salt buffer, then DNA that remained bound was eluted and analyzed by gel electrophoresis.

In the absence of protein, or in the presence of Mis4^{Scc2}/Ssl3^{Scc4} only, no DNA was recovered (Fig. 2d). About 5% of input DNA was recovered when we performed the reaction in the presence of cohesin. The amount of bound DNA increased 5-fold when also Mis4^{Scc2}/Ssl3^{Scc4} was included. This suggests that the cohesin loader promotes salt-resistant cohesin loading onto DNA. The bulk of DNA binding occurred within an hour, followed by a slower increase up to four hours (Fig. 2e). DNA binding in the absence of Mis4^{Scc2}/Ssl3^{Scc4} similarly increased over time, albeit at a lower level, indicating that it might also be the consequence of an active loading process. The salt-resistant loading onto DNA required that the incubation itself was performed at low salt concentrations, excluding the possibility of a high salt artifact (Extended Data Fig. 3a). Both Mis4^{Scc2} and the Mis4^{Scc2}/Ssl3^{Scc4} complex caused indistinguishable concentration-dependent stimulation of cohesin loading (Fig. 2f), suggesting that the activities to load cohesin onto DNA are contained within the Mis4^{Scc2} subunit of the cohesin loader.

Cohesin and its loader localize to specific chromosomal loci[24,25]. We modified our DNA substrate to contain fission yeast DNA sequences that are *in vivo* enriched for, or free of, Mis4^{Scc2}/Ssl3^{Scc4} and cohesin[25]. No differences were observed when comparing cohesin loading using these substrates, indicating that DNA sequence does not affect cohesin loading, at least under our *in vitro* conditions (Fig. 2g).

As expected, different closed circular DNAs served as efficient substrates in the loading reaction, but not linear DNA (Extended Data Fig. 3b). To confirm the interaction was topological, we retrieved cohesin from a loading reaction, then linearized the bound circular DNA. This released cleaved DNA into the supernatant, while residual uncleaved DNA remained cohesin-bound on the beads (Fig. 3a,b). Topological loading was also observed in a loading reaction containing the Mis4^{Scc2} subunit only (Extended Data Fig. 3c). The lower level of DNA loaded onto cohesin in the absence of any loader was also released by linearization (Fig. 3b), suggesting that cohesin in principle achieves topological loading onto DNA independently of a cohesin loader, albeit inefficiently.

Cohesin dissociates from chromosomes to trigger anaphase following cleavage of its kleisin subunit by the protease separase[14,26]. To test whether our *in vitro* loaded cohesin recapitulates this, we replaced one of the two separase recognition sequences in the kleisin subunit Rad21 with a TEV protease recognition motif (Fig. 3c). After loading this modified cohesin complex, we added TEV protease. This led to efficient Rad21 cleavage and concomitant loss of DNA from TEV-cleavable cohesin, but not from cohesin lacking the TEV recognition site (Fig. 3d). Thus cohesin achieves its final, cleavage-sensitive topological state on DNA from its initial loading. We conclude that topological loading onto DNA is an intrinsic activity of the cohesin complex, although it is greatly facilitated by the Mis4^{Scc2}/Ssl3^{Scc4} cohesin loader complex, particularly the Mis4^{Scc2} subunit.

The loader engages cohesin's ATPase

To investigate the contribution of cohesin's ATPase, we carried out loading reactions in the absence or presence of ATP, ADP or non-hydrolyzable ATP analogs and found that ATP hydrolysis is required for cohesin loading onto DNA (Fig. 4a). Cohesin complexes harboring ATPase-inactivating point mutations in the Walker A ATPase motif of Psm1 or Psm3 also failed to be loaded onto DNA by Mis4^{Scc2}/Ssl3^{Scc4} *in vitro* (Fig. 4b and Extended Data Fig. 2d). Therefore the ATP hydrolysis-dependent DNA binding step that has been inferred from mutant analysis *in vivo*[19,20] is most likely that of topologically loading onto DNA.

Fission yeast cohesin hydrolyzed ATP at a rate of 3.7 min^{-1}, dependent on its intact ATPase (Fig. 4c,d). The addition of DNA or Mis4^{Scc2}/Ssl3^{Scc4} did not change this rate, but the addition of both led to a marked increase in ATP hydrolysis. This suggests that Mis4^{Scc2}/Ssl3^{Scc4} stimulates cohesin loading once the loader, cohesin and DNA come together. The Mis4^{Scc2} subunit alone had a similar effect as the loader complex. Linear DNA was as efficient as circular DNA in stimulating ATP hydrolysis (Fig. 4d), implying that DNA topology does not affect cohesin loading, but rather the retention of cohesin on DNA once loaded.

Multiple interactions around the ring

We next analyzed the physical interaction between Mis4^{Scc2}/Ssl3^{Scc4} and cohesin. Consistent with previous observations[10,20], the two purified complexes coimmunoprecipitated, suggesting that they directly interact. Mis4^{Scc2}/Ssl3^{Scc4} (or Mis4^{Scc2} by itself) also interacted with the purified Psm1/Psm3 dimer, with the Psm3 subunit alone, as well as with the purified Psc3 subunit (Extended Data Fig. 4). To map the interacting regions, we used tiling peptide arrays covering each of the four cohesin subunits. They were probed with Mis4^{Scc2}/Ssl3^{Scc4} that was subsequently detected by immunoblotting. As an example, Figure 5a shows the identification of a candidate Mis4^{Scc2}/Ssl3^{Scc4} interaction site on Psm1, close to its hinge. We identified putative loader interaction sites on all four cohesin subunits, located at positions along the cohesin ring circumference (Fig. 5b and Extended

Data Fig. 5). The contact regions within Psm1, Psm3 and Psc3 show evolutionary conservation. In particular, two of the interacting regions in Psc3 delineate the 'stromalin homology domain'[27] that is characteristic of Psc3 orthologs (Extended Data Fig. 6a-c).

A second set of peptide arrays was used to identify amino acids critical for these interactions. To verify the importance of the key residues identified (Extended Data Fig. 6d-f), we made corresponding point mutations in the *psm1*$^{+}$, *psm3*$^{+}$ and *psc3*$^{+}$ genes and ectopically expressed them in fission yeast cells carrying temperature-sensitive mutations in the respective subunit (Extended Data Fig. 7). Point mutations in Psm3 and each of the three interaction sites in Psc3 caused failure to complement temperature sensitivity. In the case of Psm1, we observed sensitivity to DNA damaging agents, a known characteristic of reduced cohesin function[28]. Thus, Mis4^{Scc2}/Ssl3^{Scc4} interacts with cohesin at multiple sites around its ring circumference, at places that are important for cohesin function.

Ring contacts promote cohesin loading

The interaction of Mis4^{Scc2}/Ssl3^{Scc4} with Psc3 was of particular interest as no molecular role has yet been ascribed to this essential cohesin subunit[12-16]. The interaction between the two components was noticeably reduced by point mutations in Psc3, particularly those within the stromalin homology domain (Fig. 5c). When expressed in fission yeast, all of the interaction site mutants failed to rescue the sister chromatid cohesion defect of a *psc3-303* temperature sensitive strain (Fig. 5d), confirming that interaction of Psc3 with the cohesin loader is important for sister chromatid cohesion.

To define the role of Psc3 in cohesin loading, we carried out loading reactions with a cohesin trimer including Psm1, Psm3 and Rad21, lacking Psc3. The cohesin trimer by itself did not detectably bind RC DNA, though addition of Mis4^{Scc2}/Ssl3^{Scc4} resulted in a small degree of loading (Fig. 5e and Extended Data Fig. 8a). Adding back Psc3 to the cohesin trimer also gave a low level of DNA loading. However, Psc3 together with Mis4^{Scc2}/Ssl3^{Scc4} substantially restored cohesin loading. Likewise, DNA-dependent ATPase activity of the cohesin trimer was low, but was coordinately stimulated by addition of Psc3 and Mis4^{Scc2}/Ssl3^{Scc4} (Extended Data Fig. 8b). The rescue of cohesin loading by Psc3 was reduced by point mutations in loader interaction sites, especially those in the stromalin homology domain (Fig. 5e). This effect was augmented at a higher incubation temperature of 37 °C, when small interaction defects might be less well tolerated. Each of the loader interaction-deficient Psc3 proteins stimulated the loader-independent ATPase of the cohesin trimer to a similar extent as wild type Psc3 (Extended Data Fig. 8c), suggesting that they retain functional interactions within the cohesin complex. Thus, a specific interaction of Psc3 with Mis4^{Scc2}/Ssl3^{Scc4} is required to promote cohesin loading.

We also investigated whether interaction of Mis4^{Scc2}/Ssl3^{Scc4} with Psm1 and Psm3 contributes to cohesin loading. We introduced loader interaction site mutations into both Psm1 and Psm3 (Psm1/3^{LM}). This did not affect cohesin complex stability or its loader-independent association with DNA (Fig. 5f and Supplementary Fig. 2d). However, loading was stimulted less than 1.5-fold by Mis4^{Scc2}/Ssl3^{Scc4} while DNA loading of wild type cohesin complexes is stimulated over 4-fold by the loader. This suggests that contacts of the cohesin loader with Psm1 and Psm3 also contribute to cohesin loading.

In a complementary approach, we observed competition of the loading reaction by peptides corresponding to Mis4^{Scc2}/Ssl3^{Scc4} interaction sites on Psm1, Psm3 and Psc3. *In vitro* cohesin loading onto DNA was reduced by addition of each individual peptide, an effect that was augmented by combining the three peptides (Fig. 5g). Similar addition of peptides with a scrambled sequence, or containing point mutations that reduce the Mis4^{Scc2}/Ssl3^{Scc4}

interaction, did not elicit inhibition. Peptide addition did not affect Mis4^{Scc2}/Ssl3^{Scc4}-independent DNA loading of cohesin, indicating that the interaction site peptides target the cohesin loader. Together, our results suggest that multiple interactions of the cohesin loader along the circumference of the cohesin ring jointly promote cohesin loading onto DNA.

Discussion

We have reconstituted topological loading of cohesin onto DNA using purified fission yeast proteins. The biochemical characterization of this reaction has led to several surprises. Cohesin topologically binds to DNA independently of a loading factor or of cohesion establishment reactions. Our experiments using purified components provide final proof for the idea that cohesin entraps DNA[12], which has been previously supported by evidence from less well defined and therefore less conclusive systems[17]. A second Smc ring complex, condensin, is thought to associate with budding yeast chromatin by topological embrace[29]. Condensin binding to chromatin may not, or only in part, depend on Mis4^{Scc2}/Ssl3^{Scc4} in fission and budding yeast[30,31]. In the case of prokaryotic Smc complexes, that show striking similarity to their eukaryotic counterparts[32], a loader similar to the Mis4^{Scc2}/Ssl3^{Scc4} complex is unknown. Assuming that bacterial Smc complexes also embrace DNA, our results explain how Smc complexes can topologically bind DNA without the need for a loader. The intrinsic ability to entrap DNA also makes it possible that cohesin acts in DNA repair and transcriptional regulation by topological embrace.

Cohesin loading onto DNA *in vitro* was greatly facilitated by the cohesin loader Mis4^{Scc2}/Ssl3^{Scc4}, an essential protein complex in all eukaryotes studied. Unexpectedly, the Mis4^{Scc2} subunit alone harbored all activities required for the cohesin loading reaction. These findings contrast with the essential nature of Ssl3^{Scc4} (Refs 18,33). Budding yeast Ssl3^{Scc4} is required for protein stability of the Mis4^{Scc2} subunit *in vivo*[18]. In addition, Ssl3^{Scc4} could have a role in cohesin loading *in vivo* that was not recapitulated in our *in vitro* loading reaction. Loading occurred in a sequence non-specific fashion *in vitro*, while the cohesin loader occupies discrete locations on chromosomes *in vivo*[24,25]. In *Xenopus* egg extract, the cohesin loader is recruited to chromatin via an interaction with pre-replicative complexes that requires its Ssl3^{Scc4} subunit[34]. Ssl3^{Scc4} could mediate recruitment of the cohesin loader in the context of a chromatinized DNA substrate to ensure that cohesin loading occurs with spatial and temporal precision.

Mis4^{Scc2}/Ssl3^{Scc4} makes numerous contacts with the cohesin complex, including a prominent interaction with the previously enigmatic Psc3 subunit. These jointly facilitate cohesin loading onto DNA. By engaging into multiple contacts, Mis4^{Scc2}/Ssl3^{Scc4} could stabilize a transient conformation of the cohesin complex during the DNA loading reaction that is otherwise energetically unfavorable (Fig. 5h). Recent studies of the Smc-related DNA repair protein Rad50 have suggested how an ATP hydrolysis-dependent conformational change of the ATPase domains could be transmitted along their coiled coil[35-37]. A similar ATP-dependent conformational change has also been implicated in ring opening of a mismatch repair ABC-type ATPase[38]. Given the large dimensions of the cohesin ring, Mis4^{Scc2}/Ssl3^{Scc4} may function as a molecular “shaft” to help transmit an ATP-dependent conformational change from the head domains along the coiled coil to the hinge[39]. The Psc3 subunit in this model would act as a molecular “hitch” to connect the ATPase “engine” to the Mis4^{Scc2}/Ssl3^{Scc4} “shaft”. This scenario offers a molecular explanation for how ATP hydrolysis at the cohesin heads leads to ring opening at the opposite side of the cohesin ring. The “shaft” at the same time controls the ATPase engine to ensure it is only started when all components of the loading reaction are in place.

Full Methods

Expression and purification of Mis4^{Scc2}/Ssl3^{Scc4}

The *mis4*$^{+}$ cDNA was amplified by polymerase chain reaction (PCR) from a fission yeast *Schizosaccharomyces pombe* meiotic cDNA library (Yeast National BioResource Project, Osaka, Japan) and cloned under control of the *nmt1*$^{+}$ promoter into plasmid pREP1 (*LEU2*). An HA epitope and a protein A tag, separated by a PreScission protease recognition sequence, were added at the C-terminus, yielding plasmid pMis4PA. The *ssl3*$^{+}$ cDNA was similarly cloned under control of the *nmt1*$^{+}$ promoter, without epitope tags, into pREP2 (*ura4*$^{+}$) generating pSsl3. Both pMis4PA and pSsl3 were together introduced into fission yeast (*h*$^{-}$ *ura4-D18 leu1-32*) and protein expression induced by growing the cells in Edinburgh minimal medium (EMM2) lacking thiamine at 30 °C for 15 hours. Cell pellets were resuspended in an equal volume of CLR buffer (50 mM Tris/HCl pH 7.5, 1 mM dithiothreitol (DTT), 250 mM NaCl, 2.5 mM $MgCl_2$, 5 mM EGTA, 20% (v/v) glycerol, 0.2 mM sodium vanadate, 0.5 mM phenylmethylsulfonyl fluoride (PMSF) and a protease inhibitor cocktail (Roche)), frozen in liquid nitrogen and then broken in a freezer mill (SPEX CertiPrep 6850). The cell powder was thawed at 4 °C, then twice the volume of CLR buffer was added. The lysate was clarified at 4 °C by centrifugation at 45,000 × g for 30 minutes, then at 200,000 × g for 1 hour. The clarified lysate was mixed with IgG sepharose (GE Healthcare, 1 ml resin slurry per 50 ml of lysate) and RNase A (10 μg/ml final) at 4 °C for 3 h. The resin was washed with 15 bed volumes of R buffer (20 mM Tris/HCl pH 7.5, 0.5 mM Tris (2- carboxyethyl) phosphine hydrochloride (TCEP), 10% (v/v) glycerol, containing 250 mM NaCl and 0.5 mM PMSF, then with 15 bed volumes of the same buffer lacking PMSF. The resin was now suspended in two bed volumes of R buffer containing 250 mM NaCl, 10 μg/ml RNase A and 5 units per milliliter of PreScission protease (GE Healthcare) and incubated overnight at 4 °C. For elution, 1.5 volumes of R buffer was added to adjust the salt concentration to 100 mM NaCl and the eluate was loaded onto a HiTrap Heparin HP column (GE Healthcare). The column was developed with a linear gradient from 100 mM to 1 M NaCl in R buffer. The peak fractions were pooled and loaded onto a Superdex 200 10/300 GL gel filtration column (GE Healthcare) that was developed in R buffer containing 150 mM NaCl. The peak fractions containing Mis4/Ssl3 were concentrated to 500 μl by centrifugal ultrafiltration (Amicon Ultra, Millipore). Typically, 0.5 mg of Mis4/Ssl3 were obtained from 30 g of fission yeast cells.

The Mis4 subunit was overexpressed and purified from fission yeast (*h- ura4-D18 leu1-32*), bearing pMis4PA only, following essentially the same procedure. Typically, 0.3 mg of Mis4 were obtained from 10 g of cells.

Expression and purification of cohesin

The Psm3-encoding cDNA, fused to a 3 × Pk epitope and 7 × histidine tag at the C-terminus was cloned under control of the bidirectional budding yeast *Saccharomyces cerevisiae GAL1/GAL10* promoter in the *GAL1* direction into the shuttle vector YIplac211 (*URA3*). The cDNA encoding Psm1 was cloned into the same plasmid in the direction of the *GAL10* promoter, yielding the plasmid YIpPsm1/Psm3. The *rad21*$^{+}$ cDNA, fused to an HA epitope and a protein A tag at the C-terminus, separated by a PreScission protease recognition sequence, was cloned under control of the *GAL1* promoter into YIplac128 (*LEU2*). The *psc3*$^{+}$ cDNA, fused to a 7 × histidine tag at the N-terminus, was added in the direction of the *GAL10* promoter yielding the plasmid YIpRad21/Psc3. The linearized YIpPsm1/Psm3 and YIpRad21/Psc3 were sequentially integrated into budding yeast (*MAT*a, *ade2-1, trp1-1, can1-100, leu2,3,112, his3-11,15, ura3-52, pep4Δ::HIS3MX*) at the *URA3* and *LEU2* locus, respectively. The resultant Psm1/Psm3/Rad21/Psc3-expressing cells were grown in YP medium containing 2% raffinose to an OD_{600} = 2.0 at 30 °C. Galactose was added to the

culture at a final concentration of 2% and the cells were grown for further 4.5 hours at 30 °C. Cell pellets after centrifugation were resuspended in an equal volume of CLH buffer (50 mM HEPES/KOH pH 7.5, 1 mM DTT, 300 mM NaCl, 20% (v/v) glycerol, 0.5 mM PMSF and protease inhibitor cocktail), frozen in liquid nitrogen and broken in a freezer mill. Cell lysate preparation and purification on IgG sepharose followed the procedure for purification of Mis4/Ssl3, but CLH buffer and H buffer (25 mM HEPES/KOH pH 7.5, 0.5 mM TCEP, 10% (v/v) glycerol), containing 300 mM NaCl were used. Two volumes of R buffer were added to the eluate to bring the salt concentration to 100 mM before loading onto a HiTrap Heparin HP column. Bound proteins were eluted with steps of 300 mM, 600 mM and 1 M NaCl in R buffer. Cohesin was retrieved in the 600 mM NaCl fraction. This fraction was applied to a Superose 6 10/300 GL gel filtration column (GE Healthcare) that was developed in R buffer containing 200 mM NaCl. The peak fractions were concentrated to 400 μl by ultrafiltration. Typically, 0.5 mg of the cohesin complex was obtained from 30 g of budding yeast cells. Cohesin containing a Rad21 TEV cleavage site, cohesin bearing K38I mutations in the Walker A ATPase motif of Psm1 ($Psm1^{WA}$) or Psm3 ($Psm3^{WA}$) and the cohesin trimer lacking Psc3 were purified using the same procedure. For expression of the cohesin Psm1/3 loader interaction mutant ($Psm1/3^{LM}$, containing Psm1 K467E R468E and Psm3 R828E R829E), an additional plasmid expressing the Psm3 mutant under control of the *GAL1* promoter, based on YIplac204, was integrated at the *TRP1* locus. This plasmid also contained the budding yeast *GAL4* gene under control of the *GAL10* promoter to improve galactose-induced protein expression. Cohesin $Psm1/3^{LM}$ was purified as above.

Expression and purification of the Psm1/Psm3 heterodimer and of Psm3

For purification of the Psm1/Psm3 heterodimer, the $psm1^{+}$ cDNA was cloned into pREP1, yielding pPsm1. The $psm3^{+}$ cDNA, fused to a 3 × Pk and 7 × histidine tag at the C-terminus, was cloned into pREP2 to yield pPsm3PkH. Both proteins were simultaneously overexpressed in fission yeast and cell lysate was prepared essentially as described for Mis4/Ssl3 purification, using CLH buffer. The clarified lysate was mixed with 1 ml Ni-NTA agarose slurry (Qiagen) per 50 ml of lysate for 4 hours at 4 °C. The beads were washed with 30 volumes of H buffer containing 300 mM NaCl and the bound proteins were eluted with H buffer containing 300 mM NaCl and 250 mM imidazole. The eluate was loaded onto a Superose 6 10/300 GL gel filtration column that was developed in R buffer containing 200 mM NaCl. The peak fractions were concentrated by ultrafiltration.

Psm3 was expressed in fission yeast cells harboring the pPsm3PkH plasmid only. Purification followed the same protocol as described for the Psm1/Psm3 dimer, but Talon metal affinity resin (Clontech) was utilized for the histidine affinity purification.

Expression and purification of Psc3

The cDNA coding for Psc3, fused to a 6 × histidine tag at the N-terminus, followed by a PreScission protease recognition sequence, was cloned into the pET30a bacterial expression vector. The resulting pET30a-Psc3 was transformed into *E. coli* BL21 (DE3) Rosetta. Fresh transformants were grown in LB medium containing 50 μg/ml kanamycin and 34 μg/ml chloramphenicol to OD_{600} = 0.5 at 37 °C. 0.5 mM isopropyl β-D-1-thiogalactopyranoside (IPTG) was added and cells were further grown at 18 °C for 18 hours. Cells were harvested and resuspended in 10 pellet volumes of H buffer containing 300 mM KCl and protease inhibitors and disrupted by sonication. The lysate was clarified by centrifugation at 45,000 × g for 30 minutes at 4 °C and mixed with 1 ml Ni-NTA agarose slurry per 50 ml of the lysate for 4 hours at 4 °C. The beads were washed with H buffer containing 300 mM KCl and bound proteins were eluted in H buffer containing 300 mM KCl and 250 mM imidazole. The eluate was adjusted to 100 mM KCl and loaded onto a HiTrap Heparin HP column that was developed with a linear gradient from 100 mM to 1 M KCl in H buffer. The peak

fractions were pooled and applied to a Superdex 200 10/300 GL gel filtration column in H buffer containing 500 mM KCl. The peak fractions were dialyzed against H buffer containing 200 mM KCl and concentrated to 500 μl by ultrafiltration. Typically, 0.1 mg of his-Psc3 was obtained from 2.5 liters of culture, which was used for most of the experiments.

Alternatively, wild type and mutant versions of Psc3 were expressed and purified using pGEX-6P-1 bacterial expression vector (GE Healthcare). Expression and lysate preparation were carried out as described above, except that 100 μg/ml ampicillin instead of kanamycin was used for cell culture. The lysate was incubated with glutathione sepharose 4B (GE Healthcare) at 4 °C for 4 hours. Beads were then washed with H buffer containing 300 mM KCl and bound proteins were eluted with 20 mM glutathione in the same buffer. The eluate was treated with 5 units/ml PreScission protease at 4 °C overnight. The eluate was adjusted to 100 mM KCl in H buffer and loaded onto a HiTrap Heparin HP column. The column was developed with a linear gradient from 100 mM to 1 M NaCl in H buffer. The peak fractions were loaded onto a Superdex 200 10/300 GL gel filtration column that was developed in H buffer containing 200 mM KCl. The peak fractions containing Psc3 were concentrated to 500 μl. These preparations were used for the experiment shown in Figure 5e and Extended Data Fig. 8b,c.

For use in the protein interaction studies shown in Figure 5c and Extended Data Figure 4c, we fused the *psc3*$^{+}$ cDNA C-terminally to a 3 × Pk followed by a 7 × histidine tag (Psc3-PkH) and cloned it into the expression vector pGEX-6P-1 to yield plasmid pGEX-Psc3PkH. Protein expression, cell lysate preparation and glutathione affinity purification were carried out as above. After PreScission protease treatment, the eluate was incubated with Ni-NTA agarose at 4 °C for 4 h. Beads were washed again with H buffer containing 300 mM KCl and the bound proteins were eluted in H buffer containing 300 mM KCl and 250 mM imidazole. The eluate was adsorbed to glutathione sepharose 4B to remove residual GST, the flow-through fraction was then dialyzed against H buffer containing 300 mM KCl.

DNA, antibodies and peptides

The “covalently closed circular” (CCC) plasmid was pBluescript KSII (+). It was purified by equilibrium centrifugation in a CsCl-ethidium bromide gradient. “Relaxed circular” DNA (RC) was prepared by treating the CCC form with *E. coli* topoisomerase I (New England BioLabs). “Nicked circular” DNA (NC) was prepared by DNase I treatment of the CCC preparation in the presence of ethidium bromide. “Linear” DNA (L) was obtained from the CCC plasmid by restriction digestion using *Hin*dIII. Cohesin-bound DNA sequences from the fission yeast genome (E1, E2), and an equally sized control region (N; Ref. 25), were amplified by PCR and cloned into the *Eco*RV restriction site in pBluescript KSII (+). The coordinates of these regions on chromosome II were, E1, 256411-261337; E2, 323792-328714; N, 244641-249740. The dsDNA and Y-fork structure DNA substrate for the electrophoretic mobility shift assays were prepared by annealing 50-mer oligonucleotides, OL1+OL2 or OL1+OL3 respectively, followed by purification through polyacrylamide gel electrophoresis. The DNA sequences are listed in Supplementary Table 1. The sequences of the peptides used in the *in vitro* loading competition assay are found in Supplementary Table 2. The antibodies used for immunoprecipitation and Western blotting were, α-Pk (V5, AbD Serotec), α-HA (12C5A, Roche), α-hexameric histidine (Novagen) and α-tubulin (Cell Signaling). Antibodies raised against fission yeast Psm1, Rad21 and Mis4 were from BioAcademia.

DNA electrophoretic mobility shift assay

All indicated concentrations of the components are the final concentration in the reaction mixture. The 50-mer DNA substrates were ^{32}P-labeled at their 5′ ends using polynucleotide kinase. 10 nM of the DNA substrates and the indicated concentrations of Mis4/Ssl3 were incubated in 25 mM Tris/HCl pH 7.5, 0.5 mM TCEP, 50 mM NaCl, 0.1 mg/ml BSA and 8% (v/v) glycerol at 37 °C for 15 min. The reactions were then resolved using 5% acrylamide gel electrophoresis in 1 × TAE buffer at 4 °C. Gels were dried on DEAE paper. The gel image was visualized and band intensities were quantified using a Phosphorimager and ImageQuant software (GE Healthcare).

In vitro cohesin loading assay

The standard reaction volume was 15 μl and contained 100 nM Mis4/Ssl3 and 3.3 nM molecules of RC DNA (“Relaxed Circular” pBluescript KSII (+), see above) which were mixed on ice in CL1 buffer (35 mM Tris/HCl pH 7.5, 1 mM TCEP, 25 mM NaCl, 25 mM KCl, 1 mM $MgCl_2$, 15% (v/v) glycerol and 0.003% Tween 20). After 5 minutes, 150 nM cohesin and 100 nM Psc3 were added for further incubation on ice for 5 minutes. Free Psc3 was added to the reaction because Psc3 appeared somewhat substoichiometric in our cohesin preparations and DNA binding by cohesin slightly increased by this addition (Fig. 2b and Extended Data Fig. 3d). The loading reaction was now initiated by addition of 0.5 mM ATP followed by incubation at 32 °C for 1 hour. To stop the loading reaction and to dissociate non-topologically DNA bound cohesin, 500 μl of CP buffer (35 mM Tris/HCl pH 7.5, 0.5 mM TCEP, 500 mM NaCl, 10 mM EDTA, 5% (v/v) glycerol, 0.35% Triton X-100) was added to the reaction mixture and incubated at 32 °C for 5 minutes, followed by 5 minutes on ice. α-Pk antibody-coated, protein A-conjugated magnetic beads (Dynal Inc.) were added and rocked at 4 °C for 15 hours. The magnetic beads were washed three times with CW1 buffer (35 mM Tris/HCl pH 7.5, 0.5 mM TCEP, 750 mM NaCl, 10 mM EDTA, 0.35% Triton X-100), and then once with CW2 buffer (35 mM Tris/HCl pH 7.5, 0.5 mM TCEP, 100 mM NaCl, 0.1% Triton X-100). The beads were now suspended in 15 μl elution buffer (10 mM Tris/HCl pH 7.5, 1 mM EDTA, 50 mM NaCl, 0.75% SDS, 1 mg/ml protease K) and incubated at 50 °C for 20 minutes. The recovered DNA was analyzed by 1% agarose gel electrophoresis in 1 × TAE and the gel was stained with GelRed (Biotium). Gel images were captured using a GelDoc-It Imager (UVP) and band intensities quantified using ImageQuant.

In experiments that included linearization of cohesin-bound RC DNA, the cohesin-bound DNA was retrieved by α-Pk immunoprecipitation as described above, except that EDTA was omitted from the CP and CW buffers. The magnetic beads were further washed with RE buffer (35 mM Tris/HCl pH 7.5, 0.5 mM TCEP, 100 mM NaCl, 10 mM $MgCl_2$, 0.1 mg/ml BSA, 0.1% Triton X-100). The beads were incubated with *Pst*I (20 units, NEB) in 10 μl RE buffer at 10 °C for 3 hours. The salt concentration was now adjusted to 500 mM NaCl in 15 μl and the reaction mixture was incubated on ice for 10 minutes, before the DNA molecules in the supernatant and bead fractions were analyzed as described above.

The cleavage of engineered Rad21 by TEV protease was carried out at 16 °C for 2 h. TEV protease (10 units, Invitrogen) was added to the reaction mixture following the cohesin loading reaction. The cohesin-bound DNA was analyzed as above.

The cohesin loading reactions using cohesin trimer and Psc3 mutants were carried out in the standard reaction condition with sight modification. 100 nM Mis4/Ssl3 was initially mixed with RC DNA, then 150 nM cohesin trimer and 150 nM Psc3 were added. The reaction mixture was incubated at the indicated temperature for 10 min, then the reaction was

initiated by addition of 0.5 mM ATP. After 1 hour incubation at the indicated temperature, cohesin-bound DNA was analyzed as described above.

For the peptide competition experiments, the cohesin loading reaction was carried out in CL2 buffer (50 mM Tris/HCl pH 7.5, 1 mM TCEP, 25 mM NaCl, 1 mM $MgCl_2$, 15% (v/v) glycerol, 0.003% Tween 20). The indicated peptides (Psm1 peptides, 100 μM; Psm3 peptides, 100 μM; Psc3-1 peptides 50 μM) were included with 50 nM Mis4/Ssl3 and 3.3 nM RC DNA for incubation on ice for 10 minutes, before 100 nM cohesin and 0.5 mM ATP were added to the reaction mixture for incubation at 32 °C for 45 minutes. Cohesin-bound DNA was then analyzed as above.

ATPase assay

150 nM cohesin, 100 nM Mis4/Ssl3 and 3.3 nM RC DNA were mixed in CL1 buffer on ice. For the analyses of the cohesin trimer, 150 nM cohesin trimer, 100 nM Mis4/Ssl3, 150 nM Psc3 and 3.3 nM RC DNA were used. Note that no detectable ATP hydrolysis was observed in the absence of cohesin or cohesin trimer (Figure 4c and data not shown). Reactions were initiated by addition of 0.25 mM ATP, spiked with [γ-^{32}P]-ATP (PerkinElmer), and incubated at 32 °C. Reaction aliquots were retrieved at 0, 15, 30 and 60 minutes and terminated by addition of 3 volumes of 500 mM EDTA. 1 μl of the terminated reactions were spotted on polyethylenimine cellulose F sheets (Merck), and separated by thin layer chromatography using 400 mM LiCl in 1 M formic acid as the mobile phase. The separated spots representing ATP and released inorganic phosphate were quantified using a Phosphorimager and ImageQuant software.

Protein interaction analyses

For coimmunoprecipitation, 50 nM Mis4/Ssl3 and 50 nM cohesin or cohesin subunits (Psm1/Psm3 dimer, Psm3 or Psc3-PkH) were mixed in 50 μl of IP buffer (25 mM Tris/HCl pH 7.5, 0.5 mM TCEP, 100 mM NaCl, 2.5 mM $MgCl_2$, 0.2% Triton X-100 and 5% (v/v) glycerol) containing 0.5 mg/ml BSA and incubated at 25 °C for 15 minutes. After placing on ice for 15 minutes, the binding mixtures were transferred to α-Pk antibody-coated, protein A-conjugated magnetic beads and rocked overnight at 4 °C. The beads were washed three times with IP buffer. The bound proteins were eluted in SDS-polyacrylamide gel electrophoresis (SDS-PAGE) loading buffer, separated by 8.5% SDS-PAGE and detected by Western blotting using α-HA antibody to detect Mis4 and α-Pk to detect Psm3 or Psc3. For far Western analysis, purified cohesin proteins were separated by SDS-PAGE, and transferred to a nitrocellulose membrane. The transferred proteins were renatured in FW buffer (25 mM HEPES/KOH pH 7.5, 150 mM KCl, 15 mg/ml BSA, 0.05% Tween 20) at room temperature for 2 hours. The membranes were then blocked in FW buffer containing 5% milk powder. After rinsing with FW buffer, the membrane was incubated with 2.5 μg/ml Mis4/Ssl3 in FW buffer at 4 °C for 15 hours. Bound Mis4/Ssl3 was detected by probing with an α-HA antibody. For the interaction studies using tiling peptide arrays, 20 amino acid long peptides covering the amino acid sequences of Psm1, Psm3, Rad21 or Psc3, shifted by 2 amino acids, were synthesized on cellulose membranes using an Intavis Multipep peptide synthesizer (Intavis Bioanalytical Instruments AG). The membrane was activated in 50% methanol/10% acetic acid, then blocked with 2.5% milk powder in TBS (25 mM Tris/HCl pH 7.5, 150 mM NaCl, 0.1% Tween 20) at room temperature for 2 hours. The blocked membrane was incubated with 1 μg/ml Mis4/Ssl3 in TBS buffer at 4 °C for 15 hours. The membrane was washed with TBS and bound Mis4/Ssl3 was detected using an α-HA antibody.

Europe PMC Funders Author Manuscripts

Fission yeast strain, media and genetic methods

Standard methods were used for fission yeast cell propagation and genetic manipulation as described. To investigate the consequence of mutations within the putative Mis4/Ssl3 interactions sites in cohesin, the *psm1*$^+$, *psm3*$^+$ and *psc3*$^+$ open reading frames were cloned behind their upstream promoter sequences (951 bp, 977 bp and 990 bp respectively, for *psm1*$^+$, *psm3*$^+$ and *psc3*$^+$) into the pARG1H vector. At the C-terminus, each protein was fused to a 3 × Pk followed by 7 × histidine tag to facilitate detection. The resultant plasmids formed the basis for the introduction of point mutations to alter Mis4/Ssl3 interaction sites using site-directed mutagenesis. Plasmids were linearized and integrated into the *arg1*$^+$ locus of the *psm1-897*, *psm3-602* and *psc3-303* temperature sensitive strains, respectively, obtained from the Yeast National BioResource Project. Protein expression was monitored by Western blotting of yeast whole cell extracts obtained by glass bead breakage and TCA precipitation. For analysis of temperature sensitivity and drug resistance, exponentially growing cultures were spotted in 5-fold serial dilutions on YES agar plates and grown at the indicated temperatures for 3 to 5 days.

Sister chromatid cohesion assay

The GFP-marked cen2 locus was introduced into the *psc3-303* strain, followed by the vectors carrying wild type *psc3*$^+$ or the respective loader interaction site mutant alleles. Equal Psc3 expression levels were confirmed by Western blotting. Exponentially growing cultures were shifted to 37 °C for 3 hours. Cells were fixed with 70% ethanol. Cells were photographed and the percentage of cells with split GFP signals were counted using an Axioplan 2 Imaging microscope (Zeiss) equipped with a 100x/1.45 NA objective and an Orca-ER camera (Hamamatsu). At least 100 cells were scored for each strain, the experiment was performed three times, the mean and standard deviation are shown.

Supplementary Material

Refer to Web version on PubMed Central for supplementary material.

Acknowledgments

We are grateful to N. O'Reilly for peptide synthesis, A. Alidoust and N. Patel for fermentation and J. Hurwitz, T. Toda and members of the Chromosome Segregation Laboratory for discussion and comments on the manuscript. This work was supported by the European Research Council, Y. M. was supported by the Japanese Society for the Promotion of Science (JSPS).

REFERENCES

1. Michaelis C, Ciosk R, Nasmyth K. Cohesins: Chromosomal proteins that prevent premature separation of sister chromatids. Cell. 1997; 91:35–45. [PubMed: 9335333]
2. Guacci V, Koshland D, Strunnikov A. A direct link between sister chromatid cohesion and chromosome condensation revealed through analysis of *MCD1* in S. cerevisiae. Cell. 1997; 91:47–57. [PubMed: 9335334]
3. Losada A, Hirano M, Hirano T. Identification of *Xenopus* SMC protein complexes required for sister chromatid cohesion. Genes Dev. 1998; 12:1986–1997. [PubMed: 9649503]
4. Sjögren C, Nasmyth K. Sister chromatid cohesion is required for postreplicative double-strand break repair in *Saccharomyces cerevisiae*. Curr. Biol. 2001; 11:991–995. [PubMed: 11448778]
5. Wendt KS, et al. Cohesin mediates transcriptional insulation by CCCTC-binding factor. Nature. 2008; 451:796–801. [PubMed: 18235444]
6. Musio A, et al. X-linked Cornelia de Lange syndrome owing to SMC1L1 mutations. Nat. Genet. 2006; 38:528–530. [PubMed: 16604071]

7. Solomon DA, et al. Mutational inactivation of STAG2 causes aneuploidy in human cancer. Science. 2011; 333:1039–1043. [PubMed: 21852505]
8. Losada A, Hirano T. Intermolecular DNA interactions stimulated by the cohesin complex in vitro: Implications for sister chromatid cohesion. Curr. Biol. 2001; 11:268–272. [PubMed: 11250156]
9. Onn I, Koshland D. In vitro assembly of physiological cohesin/DNA complexes. Proc. Natl. Acad. Sci. USA. 2011; 108:12198–12205. [PubMed: 21670264]
10. Bermudez VP, et al. In vitro loading of human cohesin on DNA by the human Scc2-Scc4 loader complex. Proc. Natl. Acad. Sci. USA. 2012; 109:9366–9371. [PubMed: 22628566]
11. Anderson DE, Losada A, Erickson HP, Hirano T. Condensin and cohesin display different arm conformations with characteristic hinge angles. J. Cell Biol. 2002; 156:419–424. [PubMed: 11815634]
12. Haering CH, Löwe J, Hochwagen A, Nasmyth K. Molecular architecture of SMC proteins and the yeast cohesin complex. Mol. Cell. 2002; 9:773–788. [PubMed: 11983169]
13. Tóth A, et al. Yeast Cohesin complex requires a conserved protein, Eco1p (Ctf7), to establish cohesion between sister chromatids during DNA replication. Genes Dev. 1999; 13:320–333. [PubMed: 9990856]
14. Tomonaga T, et al. Characterization of fission yeast cohesin: essential anaphase proteolysis of Rad21 phosphorylated in the S phase. Genes Dev. 2000; 14:2757–2770. [PubMed: 11069892]
15. Losada A, Yokochi T, Kobayashi R, Hirano T. Identification and characterization of SA/Scc3p subunits in the *Xenopus* and human cohesin complexes. J. Cell Biol. 2000; 150:405–416. [PubMed: 10931856]
16. Sumara I, Vorlaufer E, Gieffers C, Peters BH, Peters J-M. Characterization of vertebrate cohesin complexes and their regulation in prophase. J. Cell Biol. 2000; 151:749–761. [PubMed: 11076961]
17. Haering CH, Farcas AM, Arumugam P, Metson J, Nasmyth K. The cohesin ring concatenates sister DNA molecules. Nature. 2008; 454:297–301. [PubMed: 18596691]
18. Ciosk R, et al. Cohesin's binding to chromosomes depends on a separate complex consisting of Scc2 and Scc4 proteins. Mol. Cell. 2000; 5:1–20. [PubMed: 10678164]
19. Weitzer S, Lehane C, Uhlmann F. A model for ATP hydrolysis-dependent binding of cohesin to DNA. Curr. Biol. 2003; 13:1930–1940. [PubMed: 14614818]
20. Arumugam P, et al. ATP hydrolysis is required for cohesin's association with chromosomes. Curr. Biol. 2003; 13:1941–1953. [PubMed: 14614819]
21. Ben-Shahar TR, et al. Eco1-dependent cohesin acetylation during establishment of sister chromatid cohesion. Science. 2008; 321:563–566. [PubMed: 18653893]
22. Ünal E, et al. A molecular determinant for the establishment of sister chromatid cohesion. Science. 2008; 321:566–569. [PubMed: 18653894]
23. Sakai A, Hizume K, Sutani T, Takeyasu K, Yanagida M. Condensin but not cohesin SMC heterodimer induces DNA reannealing through protein-protein assembly. EMBO J. 2003; 22:2764–2775. [PubMed: 12773391]
24. Lengronne A, et al. Cohesin relocation from sites of chromosomal loading to places of convergent transcription. Nature. 2004; 430:573–578. [PubMed: 15229615]
25. Schmidt CK, Brookes N, Uhlmann F. Conserved features of cohesin binding along fission yeast chromosomes. Genome Biol. 2009; 10:R52. [PubMed: 19454013]
26. Uhlmann F, Wernic D, Poupart M-A, Koonin EV, Nasmyth K. Cleavage of cohesin by the CD clan protease separin triggers anaphase in yeast. Cell. 2000; 103:375–386. [PubMed: 11081625]
27. Pezzi N, et al. *STAG3*, a novel gene encoding a protein involved in meiotic chromosome pairing and location of *STAG3*-related genes flanking the Williams-Beuren syndrome deletion. FASEB J. 2000; 14:581–592. [PubMed: 10698974]
28. Birkenbihl RP, Subramani S. Cloning and characterization of *rad21* an essential gene of *Schizosaccharomyces pombe* involved in DNA double-strand-break repair. Nucl. Acids Res. 1992; 20
29. Cuylen S, Metz J, Haering CH. Condensin structures chromosomal DNA through topological links. Nat. Struct. Mol. Biol. 2011; 18:894–901. [PubMed: 21765419]

30. D'Ambrosio C, et al. Identification of *cis*-acting sites for condensin loading onto budding yeast chromosomes. Genes Dev. 2008; 22:2215–2227. [PubMed: 18708580]
31. Furuya K, Takahashi K, Yanagida M. Faithful anaphase is ensured by Mis4, a sister chromatid cohesion molecule required in S phase and not destroyed in G_1 phase. Genes Dev. 1998; 12:3408–3418. [PubMed: 9808627]
32. Gruber S, Errington J. Recruitment of condensin to replication origin regions by ParB/SpoOJ promotes chromosome segregation in *B. subtilis*. Cell. 2009; 137:685–696. [PubMed: 19450516]
33. Bernard P, et al. A screen for cohesion mutants uncovers Ssl3, the fission yeast counterpart of the cohesin loading factor Scc4. Curr. Biol. 2006; 16:875–881. [PubMed: 16682348]
34. Takahashi TS, Basu A, Bermudez V, Hurwitz J, Walter JC. Cdc7-Drf1 kinase links chromosome cohesion to the initiation of DNA replication in *Xenopus* egg extracts. Genes Dev. 2008; 22:1894–1905. [PubMed: 18628396]
35. Lammens K, et al. The Mre11:Rad50 structure shows an ATP-dependent molecular clamp in DNA double-strand break repair. Cell. 2011; 145:54–66. [PubMed: 21458667]
36. Williams GJ, et al. ABC ATPase signature helices in Rad50 link nucleotide state to Mre11 interface for DNA repair. Nat. Struct. Mol. Biol. 2011; 18:423–431. [PubMed: 21441914]
37. Lim HS, Kim JS, Park YB, Gwon GH, Cho Y. Crystal structure of the Mre11-Rad50-ATPγS complex: understanding the interplayy between Mre11 and Rad50. Genes Dev. 2011; 25:1091–1104. [PubMed: 21511873]
38. Warren JJ, et al. Structure of the human MutSα DNA lesion recognition complex. Mol. Cell. 2007; 26:579–592. [PubMed: 17531815]
39. Nasmyth K. Cohesin: a catenase with separate entry and exit gates? Nat. Cell Biol. 2011; 13:1170–1177. [PubMed: 21968990]

Europe PMC Funders Author Manuscripts

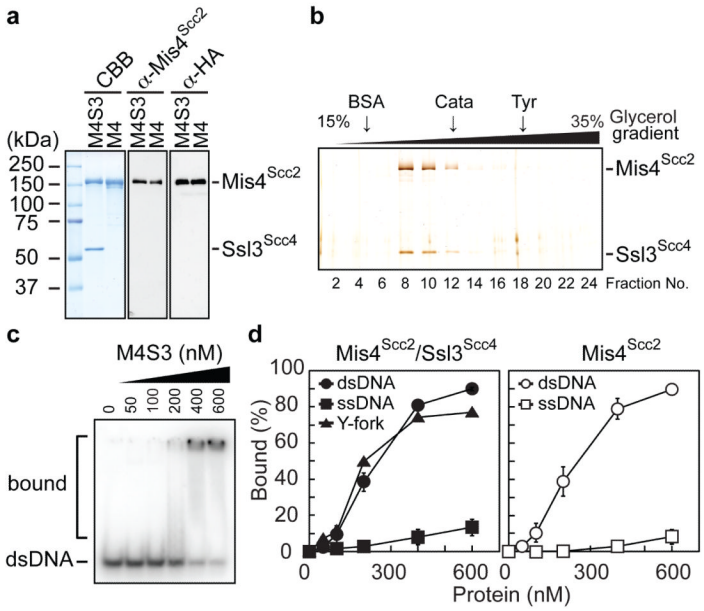

Figure 1. Mis4^{Scc2}/Ssl3^{Scc4} is a DNA binding protein

a, Purified Mis4^{Scc2}/Ssl3^{Scc4} complex (M4S3) and its Mis4^{Scc2} subunit (M4) were analyzed by SDS-PAGE and Coomassie blue staining (CBB) or Western blotting using antibodies directed against Mis4 or its C-terminal HA epitope. **b**, glycerol gradient centrifugation of the Mis4^{Scc2}/Ssl3^{Scc4} complex, followed by SDS-PAGE and silver staining. Bovine serum albumin (BSA), catalase (Cata) and thyroglobulin (Tyr) were size markers. **c**, DNA binding of Mis4^{Scc2}/Ssl3^{Scc4}, using an electrophoretic mobility shift assay. **d**, Quantification of DNA binding by Mis4^{Scc2}/Ssl3^{Scc4} (left) and Mis4^{Scc2} (right). Mean and standard deviation from 3 experiments are shown.

Europe PMC Funders Author Manuscripts

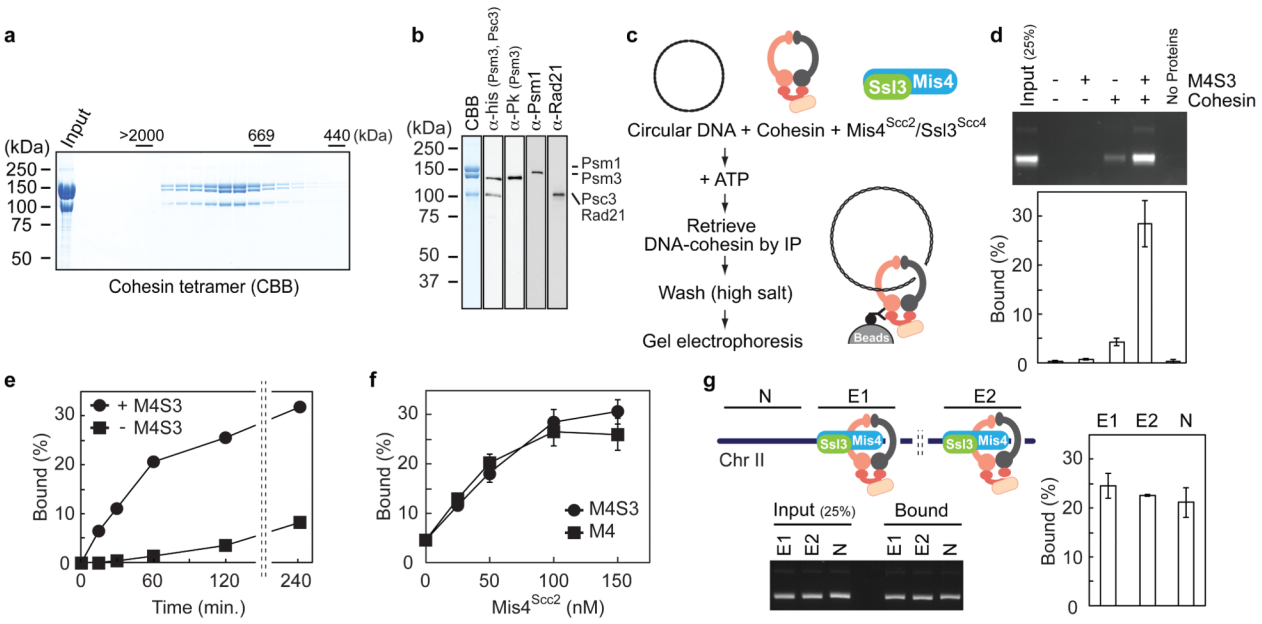

Figure 2. ***In vitro*** **reconstitution of cohesin loading onto DNA**

a, Gel filtration of the cohesin complex. **b**, Purified cohesin, analyzed by SDS-PAGE and CBB staining or Western blotting as indicated. **c**, Schematic of the cohesin loading assay. **d**, Agarose gel electrophoresis and quantification of recovered DNA during the loading reaction. **e**, Time course with or without $Mis4^{Scc2}/Ssl3^{Scc4}$ (M4S3) and **f**, Titration of $Mis4^{Scc2}/Ssl3^{Scc4}$, or $Mis4^{Scc2}$ only (M4). **g**, The loading reaction was carried out using RC DNA containing fission yeast cohesin-bound (E1, E2) or -unbound (N) sequences. Mean and standard deviation from at least 3 experiments are shown.

Europe PMC Funders Author Manuscripts

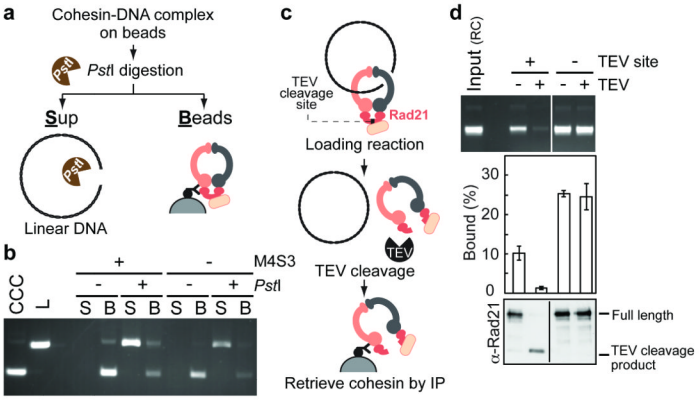

Figure 3. Topology-mediated DNA binding of cohesin

a, Schematic of the DNA release experiment. **b**, Gel image of the experiment. Covalently closed circular (CCC) input DNA and linear form (L), supernatant (S) and bead (B) fractions of experiments in presence or absence of Mis4^{Scc2}/Ssl3^{Scc4} (M4S3), with or without *Pst*I digestion, are shown. **c**, Diagram of the DNA release experiment by TEV protease (TEV) cleavage of Rad21. **d**, Agarose gel of recovered RC DNA and its quantification, the mean and standard deviation of three experiments are shown. Rad21 cleavage was monitored by Western blotting.

Europe PMC Funders Author Manuscripts

Europe PMC Funders Author Manuscripts

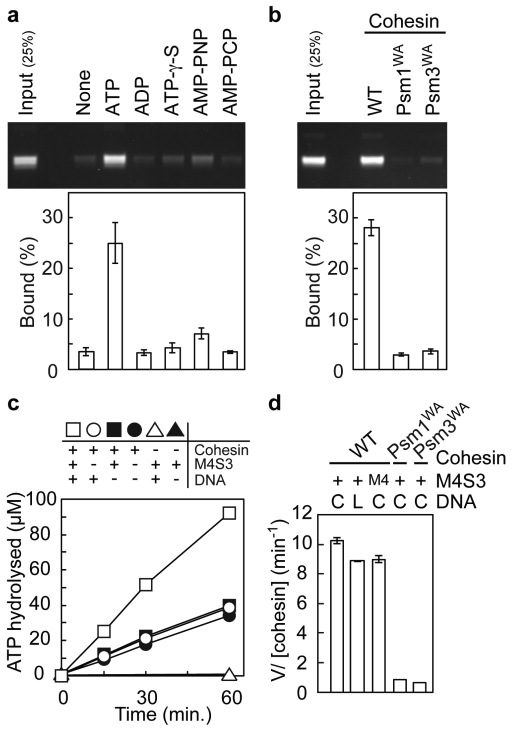

Figure 4. Mis4^{Scc2}/Ssl3^{Scc4} stimulates cohesin's ATPase

Loading reactions, **a**, in the absence or presence of ATP or derivatives, or **b**, comparing wild type or Walker A motif mutant cohesin. **c**, Timecourse analysis of ATP hydrolysis by cohesin with or without Mis4^{Scc2}/Ssl3^{Scc4} (M4S3) or RC DNA. **d**, ATP hydrolysis rates of wt and mutant cohesin derived from similar timecourse analyses. RC DNA (C) or linear DNA (L) and a reaction with Mis4^{Scc2} only (M4) was included. The mean and standard deviation of three experiments are shown.

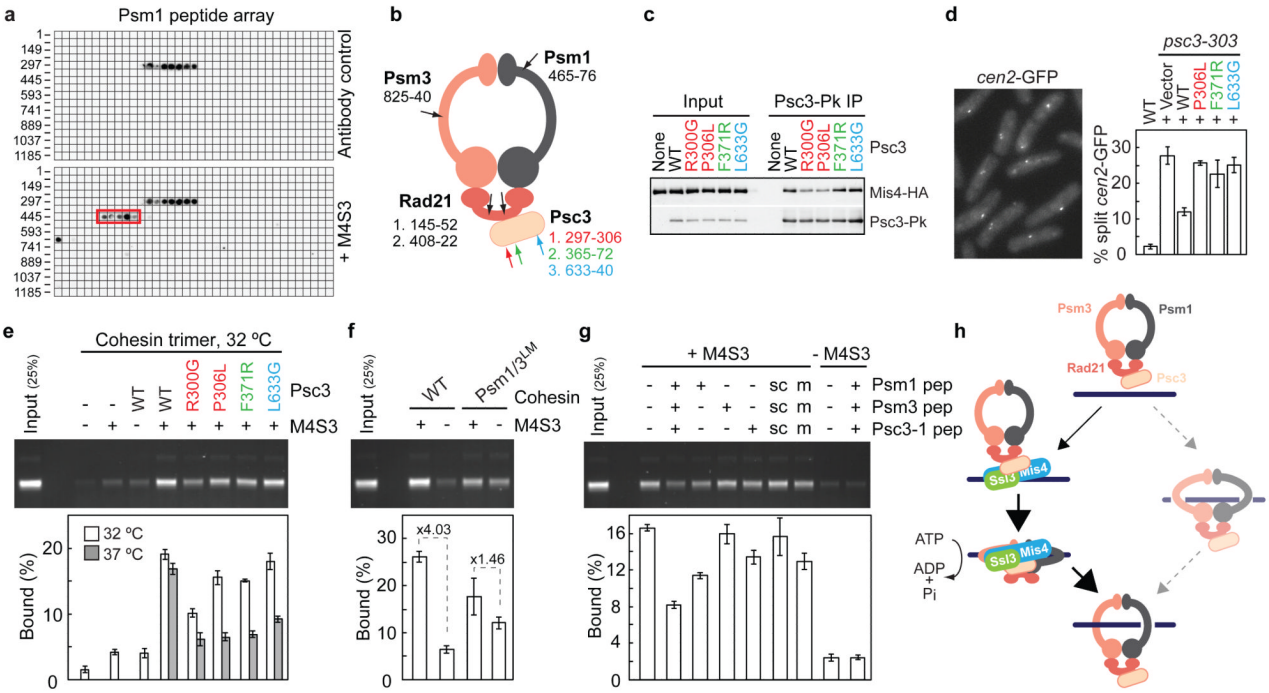

Figure 5. Mis4^{Scc2}/Ssl3^{Scc4} interactions around the cohesin ring

a, Identification of a Mis4^{Scc2}/Ssl3^{Scc4} interaction site on a Psm1 tiling peptide array. Starting positions of the first peptide in every other row are indicated. **b**, Summary of Mis4^{Scc2}/Ssl3^{Scc4} interaction sites on the four cohesin subunits **c**, Coimmunoprecipitation of wt and interaction site mutant Psc3-Pk with Mis4^{Scc2}/Ssl3^{Scc4}. **d**, Rescue of sister chromatid cohesion after *psc3-303* inactivation by wild type or interaction site mutant Psc3. **e**, Loading reactions of a cohesin trimer were supplmented with wild type or interaction site mutant Psc3. **f**, Wild type and Psm1/3^{LM} cohesin complexes were compared. **g**, Wild type (+), scrambled (sc) or point mutant (m) peptides corresponding to Mis4^{Scc2}/Ssl3^{Scc4} interactions sites were included in loading reactions. All panels present the means and standard deviations from 3 independent experiments. **h**, Model for cohesin loading onto DNA.

Europe PMC Funders Author Manuscripts